engineering proceedings

MDPI

Proceedings Paper

Symmetrical Six-Phase Induction Motors' Stator Faults Diagnostics Approach, Immune to Unbalanced Supply Voltage, Based on the Analysis of the Midpoint Electrical Potential of the Stator Star †

Hugo R. P. Antunes [1,*], Davide S. B. Fonseca [1] and Antonio J. Marques Cardoso [1]

[1] CISE—Electromechatronic Systems Research Centre, University of Beira Interior, Calçada Fonte do Lameiro, P-6201-001 Covilhã, Portugal; davide.fonseca@ieee.org (D.S.B.F.); ajmcardoso@ieee.org (A.J.M.C.)

* Correspondence: hugo.antunes@ubi.pt

† Presented at 1st International Electronic Conference on Machines and Applications, 15–30 September 2022; Available online: https://iecma2021.sciforum.net.

Abstract: The distinction of inter-turn short circuit faults (ITSCF) from abnormal conditions, such as an unbalanced voltage supply condition, has been challenging over the last few years. The asymmetries caused by both conditions are similar, and the detection of ITSCF becomes a difficult task. An ITSCF diagnostic approach based on the analysis of the electrical potential of the midpoint of the stator star, in a symmetrical six-phase induction motor (S6PIM) supplied by unbalanced voltages, is addressed in this paper. Simulation results, covering different load torques, unbalanced supply voltage levels, and fault severities, are presented in order to prove the effectiveness of the proposed technique.

Keywords: multi-phase induction motor; fault diagnosis; stator faults; inter-turns short-circuit; unbalanced supply voltage; modelling; midpoint electrical potential

Citation: Antunes, H.R.P.; Fonseca, D.S.B.; Cardoso, A.J.M.; Marques Cardoso, A.J. Symmetrical Six-Phase Induction Motors' Stator Faults Diagnostics Approach, Immune to Unbalanced Supply Voltage, Based on the Analysis of the Midpoint Electrical Potential of the Stator Star. *Eng. Proc.* **2022**, *3*, x. https://doi.org/10.3390/xxxxx

Published: date: 15 September 2022

Publisher's Note: MDPI stays neutral with regard to jurisdictional claims in published maps and institutional affiliations.

1. Introduction

Six-phase induction motors have been luring quite attention due to the high reliability and intrinsic fault-tolerance, especially the one with symmetrical winding layout, since it provides enhanced fault-tolerance [1–3].

Representing approximately 60 percent of the total faults that occur in the mid-power electric motors, ITSCF have been the most challenging fault to diagnose in an electric motor [4,5], especially when they occur simultaneously with unbalanced supply voltage or load variations conditions. Whenever these conditions take place, the existing online fault diagnostic methods have demonstrated difficulties in detecting short-circuit faults since the unbalanced supply voltage condition shares the same symptom as the ITSCF, and the load variations makes imperceptible the ITSCF during the transient periods [6,7].

One of the simplest and most robust techniques, which can be used to diagnose appropriately the ITSCF, is the analysis of the midpoint electrical potential of the stator star, which has been already proposed in the literature. Indeed, in [8], an inter-turn short circuit fault is detected in three-phase permanent magnet synchronous motors, under balanced conditions. A discrimination between both ITSCF and demagnetizing faults is analyzed in [9]. The detection of broken rotor bars and ITSCF in a tree-phase induction motor is carried out in [10]. In [11,12], the discrimination between both ITSCF and unbalance supply voltage conditions is made by combining the zero-sequence component with the high frequency injection method. The discrimination between ITSCF and high

resistive connections, performed in a nine-phase permanent magnetic synchronous machine, is reported in [13]. All these works present effective results regarding the severity degree of ITSCF. However, the exploitation of the phase fault location is only approached in [14], and the ITSCF diagnostics based on the analysis of the midpoint electrical potential of the stator star under unbalance supply voltage condition is not addressed.

This paper reports on the diagnostics of ITSCF under the presence of unbalanced supply voltages through the analysis of the midpoint electrical potential of the stator star. Both fault severity factor and faulty phase angle are analyzed from the measured data of a S6PIM, operating under unbalanced supply voltage condition, and at different load torque levels. The presented simulation results confirm the effectiveness of the technique for different severity levels and faulty phases.

2. Symmetrical Six Phase Induction Motor Model Featuring Inter-Turn Short-Circuit Faults

The occurrence of an ITSCF in phase A winding of the S6PIM is characterized in Figure 1, where phase A winding is divided into a healthy part (N_{Ah}) and a faulty part (N_{Asc}), and a fault contact resistor (R_k) is connected, in parallel, between the faulty turns.

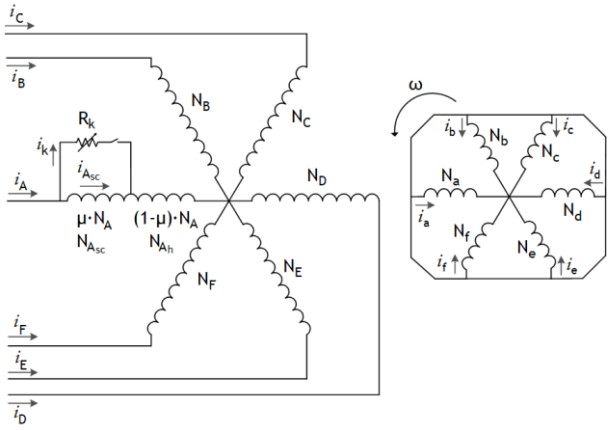

Figure 1. Schematics of the S6PIM containing an ITSCF in phase A winding.

Considering the steady-state reference frame (*abcdef*), and the phase shift of 60 degrees between phases, the equations of the S6PIM are described as [15]:

$$\begin{cases} \left[u_{ABCDEF(k)}\right] = [R_s] \cdot \left[i_{ABCDEF(k)}\right] + \dfrac{d}{dt}\left[\Psi_{ABCDEF(k)}\right] \\ 0 = [R_r] \cdot \left[i_{abcdef}\right] + \dfrac{d}{dt}\left[\Psi_{abcdef}\right] \\ T_{em} = p \cdot \left[i_{ABCDEF(k)}\right]^T \cdot \left(\dfrac{\partial}{\partial \omega_s t}\left[L_{SR(k)}\right]\right) \cdot \left[i_{abcdef}\right] \\ \dfrac{\partial \omega_m}{\partial t} = \dfrac{1}{J}(T_{em} - T_{Load} - T_{av}) \end{cases} \quad (1)$$

where the stator and rotor circuits are characterized in the first and the second equation, respectively, and the dynamic mechanical balance in the shaft is described by the last to equations. In (1), $[u_{ABCDEF}]$, $[i_{ABCDEF}]$, and $\left[i_{abcdef}\right]$ are the stator phase voltages and the stator and rotor phase currents vectors, respectively, $[R_s]$ and $[R_r]$ are the stator and rotor resistance matrix, respectively, $[\Psi_{ABCDEF}]$ and $\left[\Psi_{abcdef}\right]$ are the flux linkage matrices of the stator and rotor, respectively, p is the number of poles pair, ω_s is the synchronous angular speed, ω_m is the mechanical angular speed, J is the moment of inertia, and T_{em}, T_{Load} and T_{fv}, are the electromechanical torque, load torque, and the torque for self-ventilation and friction, respectively.

3. Analysis of the Midpoint Electrical Potential of the Stator Star for Fault Diagnostics

When a motor is star connected, each motor phase is supplied by the following voltages:

$$u_A = v_A - v_0;\ u_B = v_B - v_0;\ \cdots;\ u_F = v_F - v_0 \tag{2}$$

where, ideally, the midpoint electrical potential (v_0) is null when the motor is operating healthy. However, in the event of an ITSCF or an unbalanced supply voltage condition, v_0 is no longer null due to the asymmetry generated by these conditions.

Considering the fault current (i_k), the short-circuit turns ratio (μ) and the source voltages (v_x), the midpoint electrical potential of the stator star is deducted as follows [15]:

$$v_0 = \frac{v_A + v_B + v_C + v_D + v_E + v_F}{6} + \frac{\mu R_s i_k}{6} \tag{3}$$

If the motor is fed by a balanced supply voltage, and an inter-turn short-circuit fault occurs, ideally, the first term of the Equation (3) is null and v_0 is equal to the fault-related term. On the other hand, the first term is only affected by the presence of an unbalanced supply voltage condition. Thus, it is possible to isolate the fault related term by the following subtraction:

$$v_0 - \frac{v_A + v_B + v_C + v_D + v_E + v_F}{6} = \frac{\mu R_s i_k}{6} \tag{4}$$

and an ITSCF can be detected regardless of whether there is an unbalance supply voltage condition or not. A sinusoidal wave oscillating at the fundamental frequency results from (4), whose both amplitude and phase angle are affected as a function of the fault severity.

The amplitude of the fault-related component at the fundamental frequency, as well as its phase angle, can be determined through the application of the Fast Fourier Transform. Therefore, the severity factor (SF) and the faulty phase angle (FPA) are defined as follows:

$$\begin{cases} \dfrac{\mu R_s i_k}{6} = \hat{v}_{sc} \sin(2\pi f - \theta_v) \\ SF\ (f) = \hat{v}_{sc} \\ FPA\ (f) = \theta_v \end{cases} \tag{5}$$

where $\hat{v}_{sc}$ is the voltage peak value of fault-related component, f is the fundamental frequency (50 Hz) and θ_v is the phase angle.

Therefore, the presence of an ITSCF increases the amplitude of $\hat{v}_{sc}$ and the angle of θ_v is related to the faulty phase.

4. Results and Discussion

To validate the effectiveness of the fault diagnostic technique, the model and the fault diagnostic technique were implemented in *Matlab*/*Simulink* software, as shown in Figure 2. The S6PIM is fed by a three-phase system, under balanced and unbalanced supply voltage condition. The detailed features and parameters of this machine, as well as the validation of model, including the ITSCF, are presented in [15]. A resistor is connected in series with the motor phase A winding to cause a resistive unbalance supply voltage. Its value is adjusted so as to decrease the voltage in 4% of the rated supply voltage (150 V).

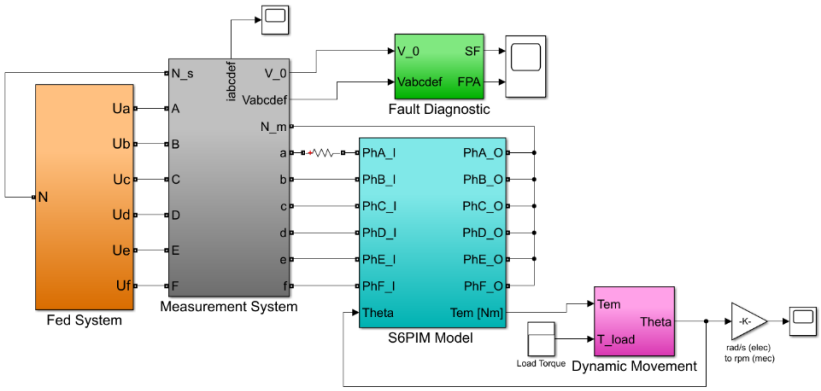

Figure 2. Matlab/Simulink model of the S6PIM, for the diagnostic of the ITSCF.

The inter-turn short circuit was performed considering four scenarios of severity (6, 12, 19, and 23 shorted turns of 138 turns per phase) with a fault contact resistance value of 0.5 Ω. The fault was also applied in different phase windings.

Figure 3 presents the simulation results for the S6PIM with ITSCF in phase A winding, for two load levels (no load and 16 Nm load torque). Figures 3a,b depict the SF as a function of the number of shorted turns, for the cases of balanced and unbalanced supply voltage condition, respectively. As expected, the SF increases as the fault becomes more severe, and the values are practically the same for both conditions, and both load levels, proving the immunity against both unbalanced supply voltage condition and load variations. Figures 3c,d display the FPA for the cases of balanced and unbalanced supply voltage condition, respectively. The FPA of both figures demonstrate slight differences between the two different load torques since the increase of the load torque introduces a deviation in the phase angle of the phase A current, which in turn affects the fault current. Nevertheless, it is not problematic for the location of the faulty phase as the behavior of both curves are identical. The presented decreasing behavior has to do with the way of the motor rotation. Though, for a better understanding of the location of the faulty phase, it is important to compare the behavior of the FPA when an ITSCF occurs in a different phase winding (phase B, C, D, E or F). This comparison is presented in Figures 4a,b.

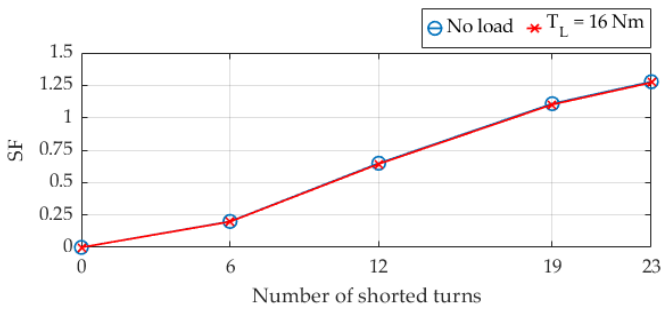

(**a**)

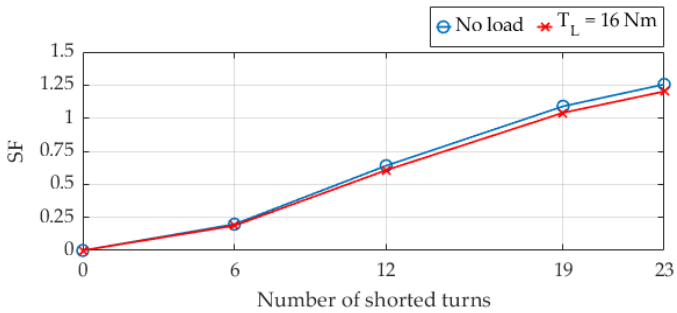

(**b**)

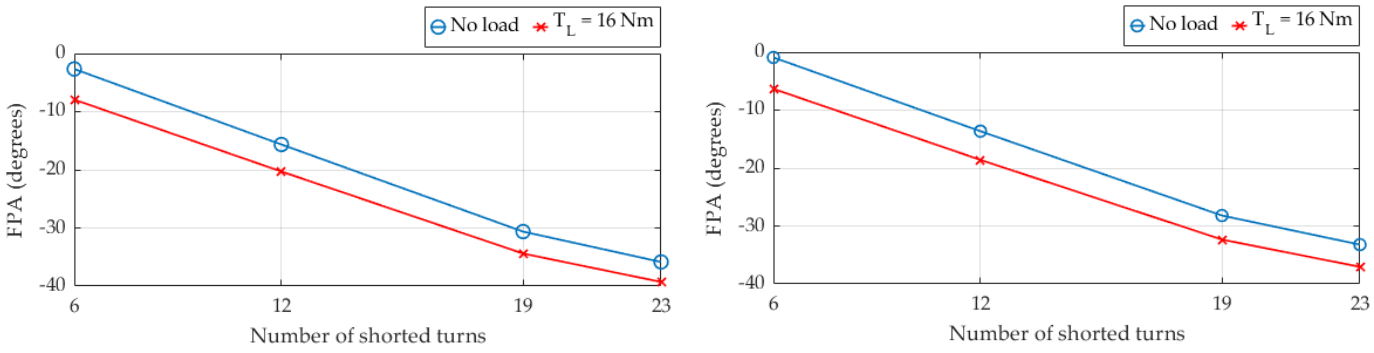

Figure 3. SF and FPA as a function of the number of the shorted turns of the phase A winding, for the motor operation at no load and 16 Nm load torque: (**a**) SF for the case of the motor operating under balanced supply voltage; (**b**) SF for the case of the motor operating under unbalanced supply voltage of 4% of the rated voltage; (**c**) FPA for the case of the motor operating under balanced supply voltage; (**d**) FPA for the case of the motor operating under unbalanced supply voltage of 4% of the rated voltage.

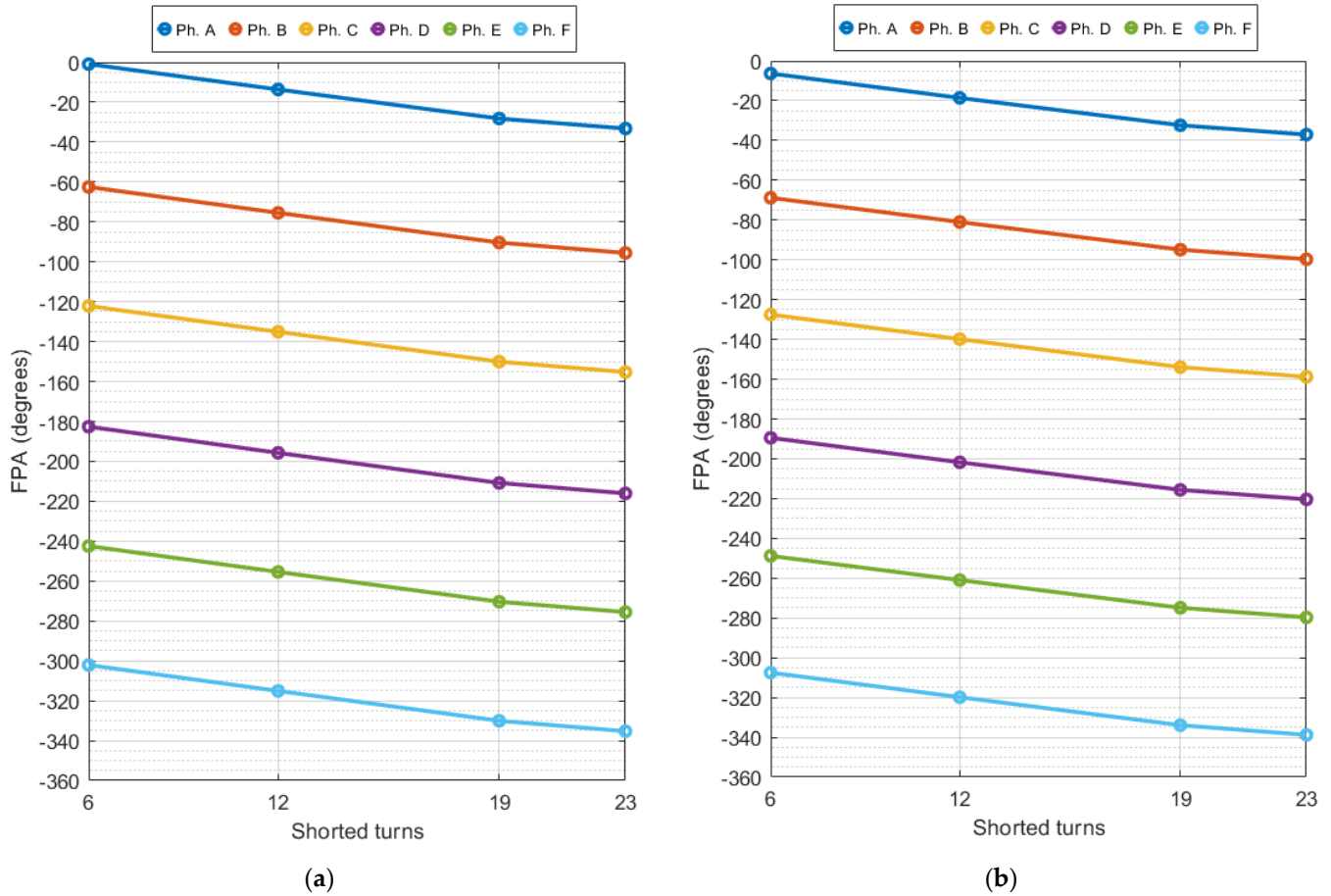

Figure 4. FPA for the occurrence of ITSCF in each phase winding for the condition of unbalanced supply voltage of 4% of the rated voltage, and a fault resistor of 0.5 Ω: (**a**) case of the motor operating at no load; (**b**) case of the motor operating at 16 Nm load torque.

Figure 4 show the FPA for the case of the occurrence of an ITSCF in the different motor phase windings, individually, for a fault resistor of 0.5 Ω. Besides, Figures 4a,b include data for the motor operation at no-load and 16 Nm load torque, respectively, under unbalanced supply voltage condition (4% of the rated voltage) introduced in phase A. As can be seen, the FPAs are very distinctive for different faulty phases. Besides, they

also decrease in the same proportion as the number of shorted turns increase. Despite of this behavior, the FPA remains very distinctive between both phases. In effect, the difference between the FPA of all phases is always nearly 60 degrees for the different fault severities, which means that the phase shift is respected.

4. Conclusions

This paper reports on the diagnostics of ITSCF under the presence of unbalanced supply voltages through the analysis of the midpoint electrical potential of the stator star. This technique cancels the effect caused by the unbalance supply voltage condition by subtracting the source voltages to the midpoint electrical potential, as it is presented in (4). Hence, the fault-related component can be easily determined. Although the necessity to have access to the midpoint of the stator is taken as a drawback, the results show that the reliability and robustness of the technique can be clearly seen as an advantage.

Possible future topics can be focused on the discrimination between other types of faults, such as eccentricity, broken rotor bars, bearing faults, etc, and the immunity of the technique under different abnormal conditions, such as load fluctuations.

Author Contributions: Conceptualization, H.R.P.A., D.S.B.F. and A.J.M.C.; methodology, H.R.P.A., D.S.B.F. and A.J.M.C.; software, H.R.P.A. and D.S.B.F.; validation, H.R.P.A. and D.S.B.F.; formal analysis, H.R.P.A and D.S.B.F.; investigation, H.R.P.A., D.S.B.F. and A.J.M.C.; resources, A.J.M.C.; data curation, H.R.P.A. and D.S.B.F; writing—original draft preparation, H.R.P.A.; writing—review and editing, D.S.B.F. and A.J.M.C.; visualization, H.R.P.A, D.S.B.F. and A.J.M.C.; supervision, A.J.M.C.; project administration, A.J.M.C.; funding acquisition, A.J.M.C. All authors have read and agreed to the published version of the manuscript.

Funding: This work was supported by National Funds through the FCT—Portuguese Foundation for Science and Technology, under Projects UIDB/04131/2020, UIDP/04131/2020, and UI/BD/153572/2022.

Conflicts of Interest: The authors declare no conflict of interest.

References

1. Levi, E. Multiphase electric machines for variable-speed applications. *IEEE Trans. Ind. Electron*. **2008**, *55*, 1893–1909.
2. Yepes, A.G.; Lopez, O.; Gonzalez-Prieto, I.; Duran, M.; Doval-Gandoy, J. A comprehensive survey on fault tolerance in multiphase ac drives, Part 1: General overview considering multiple fault types. *Machines* **2022**, *10*, 3.
3. Baneira, F.; Doval-Gandoy, J.; Yepes, A.G.; Lopez, O.; Perez Estevez, D. Control strategy for multiphase drives with minimum losses in the full torque operation range under single open-phase fault. *IEEE Trans. Power Electron*. **2017**, *32*, 6275–6285.
4. Cardoso, A.J.M. *Diagnosis and Fault Tolerance of Electrical Machines and Power Electronics*; The Institution of Engineering and Technology: London, UK, 2018.
5. Bento, F.J.F.; Adouni, A.; Muxiri, A.C.P.; Fonseca, D.S.B.; Cardoso, A.J.M. On the Risk of Failure to Prevent Induction Motors Permanent Damage, Due to the Short Available Time-to-Diagnosis of Inter-Turn Short-Circuit Faults. *IET Electr. Power Appl.* **2021**.
6. Frosini, L. Monitoring and Diagnostics of Electrical Machines and Drives: a State of the Art. In Proceedings of the 2019 IEEE Workshop on Electrical Machines Design, Control and Diagnosis (WEMDCD), Athens, Greece, 22–23 April 2019, pp. 169–176.
7. Das, S.; Purkait, P.; Koley, C.; Chakravorti, S. Performance of a load-immune classifier for robust identification of minor faults in induction motor stator winding. *IEEE Trans. Diel. Electron. Insul.* **2014**, *21*, 33–44.
8. Urresty, J.; Riba, J.; Romeral, L. Application of the zero-sequence voltage component to detect stator winding inter-turn faults in PMSMs. *Elec. Power Sys. Res.* **2012**, *89*, 38–44.
9. Urresty, J.; Riba, J.; Romeral, L. Influence of the Stator Windings Configuration in the Currents and Zero-Sequence Voltage Harmonics in Permanent Magnet Synchronous Motors with Demagnetization Faults. *IEEE Trans. Magn.* **2013**, *49*, 4885–4893.
10. Briz, F.; Degner, M.W.; Garcia, P.; Dicz, A.B. Induction machine diagnostics using zero sequence component. In Proceedings of the Fourtieth IAS Annual Meeting. Conference Record of the 2005 Industry Applications Conference, Hong Kong, China, 2–6 October 2005; pp. 34–41.
11. Hu, R.; Wang, J.; Mills, A.R.; Chong, E.; Sun, Z. Detection and Classification of Turn Fault and High Resistance Connection Fault in Permanent Magnet Machines Based on Zero Sequence Voltage. *IEEE Trans. Power Electron*. **2020**, *35*, 1922–1933.
12. Zhang, J.; Xu, Z.; Wang, J.; Zhao, J.; Din, Z.; Cheng, M. Detection and Discrimination of Incipient Stator Faults for Inverter-Fed Permanent Magnet Synchronous Machines. *IEEE Trans. Ind. Electron*. **2021**, *68*, 7505–7515.

13. Hang, J.; Zhang, J.; Ding, S.; Cheng, M. Fault Diagnosis of High-Resistance Connection in a Nine-Phase Flux-Switching Permanent-Magnet Machine Considering the Neutral-Point Connection Model. *IEEE Trans. Power Electron*. **2017**, *32*, 6444–6454.
14. Hang, J.; Zhang, J.; Cheng, M.; Huang, J. Online Interturn Fault Diagnosis of Permanent Magnet Synchronous Machine Using Zero-Sequence Components. *IEEE Trans. Power Electron*. **2015**, *30*, 6731–6741.
15. Antunes, H.R.P.; Fonseca, D.S.B.; Cardoso, A.J.M. Modeling of Symmetrical Six-Phase Induction Machines Under Stator Faults. In Proceedings of the 2021 IEEE International Electric Machines & Drives Conference (IEMDC), Hartford, CT, USA, 17–20 May 2021; pp. 1–7.